Artificial neural network approach for the prediction of coating thickness in Fe-Al coatings fabricated by mechanical milling

Aykut Canakci[a*], Fatih Erdemir[a], Temel Varol[a], Sukru Ozsahin[b], Serdar Ozkaya[a]

[a]Department of Metallurgical and Materials Engineering, Engineering Faculty,
[b]Department of Industry Engineering, Engineering Faculty
Karadeniz Technical University, Trabzon, Turkey.
aykut@ktu.edu.tr

Abstract
The aim of this study was to investigate the effect of milling time, milling speed and particle size of initial powders on the coating thickness of Fe-Al intermetallic coating produced by mechanical milling using an artificial neural network (ANN). The formation of intermetallics was confirmed by X-ray diffraction analysis. Coating morphology and cross-section microstructures were evaluated using a scanning electron microscope. As a result of this study the ANN was found to be successful for predicting the coating thickness of Fe-Al intermetallic coatings. The mean absolute percentage error (MAPE) for the predicted values didn't exceed 7.46%. The ANN model can be used for predicting of coating thickness of Fe-Al intermetallic coating produced with the different milling time, milling speed and particle size.

Keywords: Artificial neural network; Fe-Al coating; mechanical milling

Mekanik Öğütme ile üretilen Fe-Al kaplamalarında kaplama kalınlığı için yapay sinir ağı yaklaşımı

[a]Metalurji ve Malzeme Mühendisliği Bölümü, Mühendislik Fakültesi,
[b]Endüstri Mühendisliği Bölümü, Mühendislik Fakültesi,
Karadeniz Teknik Üniversitesi, Trabzon, Türkiye
aykut@ktu.edu.tr

Özet
Bu çalışmanın amacı bir yapay sinir ağı modeli kullanılarak mekanik öğütme ile üretilen Fe-Al intermetalik kaplamalarının kaplama kalınlığı üzerine öğütme zamanı, öğütme hızı ve başlangıç tozlarının partikül boyutunun etkisini araştırmaktır. İntermetalik oluşumu X ışını analizi ile araştırıldı. Kaplama morfolojisi ve mikroyapı incelemeleri taramalı elektron mikroskobu ile gerçekleştirildi. Bu çalışmanın bir sonucu olarak oluşturulan tahmin modelinin Fe-Al intermetalik kaplama kalınlığının tahmininde oldukça olduğu görüldü. Tahmin değerleri için ortalama mutlak yüzde hata (MAPE) % 7.46 değerini aşmadı. Geliştirilen tahmin modeli farklı öğütme zamanı, öğütme hızı ve başlangıç toz boyutu şartlarında üretilen Fe-Al intermetalik kaplamaların kalınlıklarının tahmini için kullanılabilir.

Anahtar Kelimeler: Yapay sinir ağı, Fe-Al kaplama, mekanik öğütme

1. INTRODUCTION

Mechanical milling is a new research area with potential industrial applications for coating on steel. Mechanical milling is a practical processing route for synthesis of phases or phase mixtures. When a powder mixture is processed by mechanical milling, some part of the milled powder forms a coating film over the milling balls and on the inside wall of the container. It was recognized recently that this phenomenon could be utilized as a flexible method to coat the surface of a steel substrate. The impacts of the milling balls activate and harden the surface. They also deliver and attach the powder particles and also can initiate chemical interactions between target object and coating powder [1].

Artificial neural networks (ANNs) which possess massive parallel computing capability can map the input-output relationships. This modeling frameworks has been recently used by many authors in various fields, for example, such as modeling of powder characteristics [2], coating process [3] wear behavior of coatings [4], and oxidation behavior of coatings [5]. Though ANN models have been developed to study the modeling of various coating process, very limited efforts have been reported to predict for coating thickness in Fe-Al coatings fabricated by mechanical milling. Thus, the primary aim of this paper was to reveal the relationship among the, microstructure, coating thickness and the process parameters during Fe-Al intermetallics formation on the steel substrate obtained by mechanical milling method. The second aim of this paper was to develop a multilayered feed-forward neural network trained with the back-propagation algorithm to model the relationship between coating thickness and process parameters (i.e. milling time, milling speed and particle size of as-received powders).

2. EXPERIMENTAL

Specimens of the low-carbon steel were used as the substrate material. The steel substrate (12 mm x12 mm x3 mm) and Al 2024 powders (d_{50}: 23 μm, d_{50}: 60 μm and d_{50}: 155 μm) were charged into the vial that made of tungsten carbide of 80 ml volume. Mechanical milling was performed in a Fritsch Pulverisette 7 planetary ball mill in an Argon atmosphere using balls (10 mm in diameter) at room temperature. The rotation rates were selected as 200, 300 and 400 rpm while the ball to powder weight ratio of 10:1 was kept constant in all the experiments. The milling times of 1, 2, 4, 6, 8 and 10 h were selected, respectively. The specimens were cut from steel substrate using a cutting machine and prepared by standard metallographic procedures for characterization. The measurement of coating thickness and morphological investigation of coated steel substrates were performed by a Zeiss Evo LS10 scanning electron microscope (SEM). The phase analysis of coated samples was evaluated by X-ray diffraction (Rigaku Corporation, Japan) using CuKα radiation (1.5405 ^{o}A) operating at 30 mA and 40 kV. The XRD patterns were recorded in the 2Θ range of 20-100 ^{o}C (step size 0.02^{o} and time per step 1s).

Fig. 1 shows the ANN models containing one input layer, two hidden layers and one output layer.

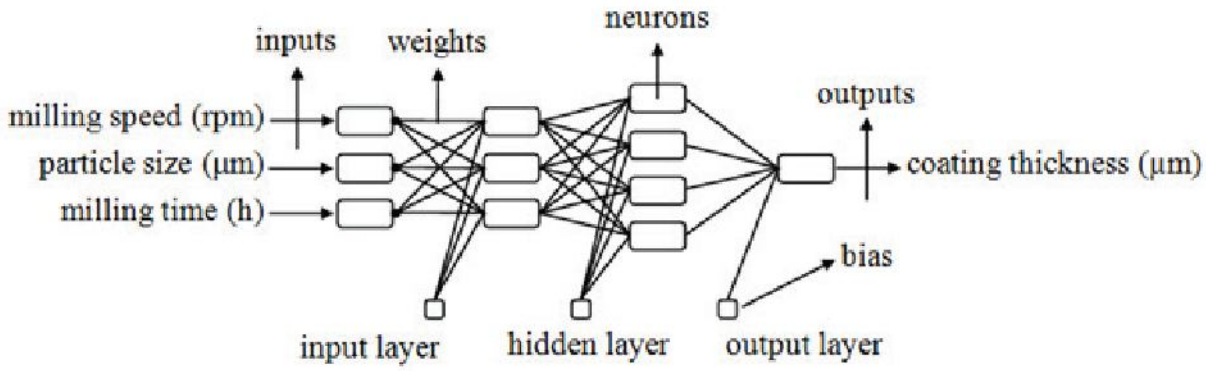


Figure 1. The ANN architecture selected as the prediction model for the coating thickness

The input layer is the first layer and is responsible for receiving the in-coming data for the ANN and for delivering the data to the intermediate layer. The hidden layer processes the information that comes from the input layer and sends it to the output layer. The neurons in the hidden layer do not have any connection to the external environment. The output layer processes the information coming from the intermediate layer and produces output data for the input layer of the network, which sends this to the outside world. Inputs (x_i) are data, obtained from the external environment or the other artificial neurons. The quantities (w_{ij}) demonstrate the effect of a data point arrives at an artificial neural cell. The addition function (threshold function, Eq.1) (net_j) calculates the net input on a neural cell. The sigmoid function (Eq.2) is the most common activation function in the ANN because it combines nearly linear behavior, curvilinear behavior, and nearly constant behavior. All of these components depend on the value of the input [6-8]. In the cell model, a bias with +1 value may increase the net input or polarization threshold input (θ_j) by a value of, -1, thereby decreasing the net input according to:

$$net_j = \sum_{i=1}^{n} x_i w_{ij} - \theta_i \qquad (1)$$

where x_i indicates the i. input, w_{ij} is the connection weight from j. element to i. element, θ_j is the polarization value (negative of the threshold value), and n indicates the sent input signal of the artificial neuron number in the previous layer. The artificial neuron output value, which depends on the selected activation function, employs a sigmoid function as the activation function [9] and is calculated using Eq. 2. The produced output is sent via network connections between different cells, as explained by:

$$y_j = f(net_j) = \frac{1}{1+e^{-net_j}} \qquad (2)$$

The processing element numbers (neurons) of the hidden layers were 3 and 4 for the model in Fig. 1. The total data are divided into two sets (67% for training data and 33% for testing data). Training and testing data was selected randomly from the experimental data set. The MATLAB software package was used for training the ANN models. The training data were used in the forecast model, as shown in Table 1.

Table 1. Experimental data and predicted output from the ANN network for training

Sample ID	Milling Speed (rpm)	Particle Size (μm)	Milling Time (h)	Coating Thickness (μm)		
				Measured	Predicted	% Error
1	200	155	1	13	13.76	-5.86
2	200	155	2	28	28.11	-0.38
4	200	155	6	50	48.90	2.21
5	200	155	8	61	62.36	-2.24
7	200	60	1	9	8.22	8.65
9	200	60	4	25	25.51	-2.03
10	200	60	6	42	39.94	4.92
12	200	60	10	66	66.61	-0.92
14	200	23	2	13	12.49	3.95
15	200	23	4	17	18.75	-10.28
17	200	23	8	40	38.97	2.58
18	200	23	10	53	53.72	-1.36
20	300	155	2	30	30.06	-0.19
21	300	155	4	36	36.33	-0.92
23	300	155	8	145	146.58	-1.09
24	300	155	10	188	186.12	1.00
25	300	60	1	15	12.13	19.14
26	300	60	2	21	20.63	1.78
28	300	60	6	90	88.58	1.57
29	300	60	8	130	133.98	-3.06
31	300	23	1	9	11.05	-22.82
33	300	23	4	21	19.82	5.60
34	300	23	6	75	76.20	-1.60
36	300	23	10	157	155.08	1.22
37	400	155	1	30	30.46	-1.55
39	400	155	4	110	109.35	0.59
40	400	155	6	184	185.12	-0.61
42	400	155	10	267	267.35	-0.13
44	400	60	2	31	29.43	5.05
45	400	60	4	60	60.97	-1.61
47	400	60	8	189	183.13	3.10
48	400	60	10	215	217.88	-1.34
49	400	23	1	17	16.16	4.91
50	400	23	2	21	24.42	-16.28
52	400	23	6	107	107.75	-0.70
53	400	23	8	156	157.76	-1.13
MAPE				**3.955**		
RMSE				**1.835**		

3. RESULTS AND DISCUSSION

3.1. The mechanism of intermetallics formation

During ball milling, a sudden (10^{-8} s.) increase in the temperature (up to 800 °C) and pressure (10^{10} -10^{11} dyn/cm^2) occurs in local areas (10^{-6} cm) which results in the formation of intermetallics. As the starting points of FeAl, $FeAl_3$ and Fe_2Al_5 formation are close to 520 °C, 580 °C and 650 °C, respectively. In addition, rise in increasing in the local temperature (up to 800 °C) can also allow formation of Fe-Al intermetallic compounds of Fe_3Al, Fe_2Al_5, $FeAl_2$ and FeAl [10]. The reaction between the low carbon steel substrate and the Al 2024 powder

can be examined by XRD. Fig. 2 shows the XRD spectra of coating surface, after heat treatment at 600 °C. The XRD patterns confirm the presence of both elemental Fe and Al components with amounts of Fe_3Al, Fe_2Al_5, $FeAl_2$ and FeAl.

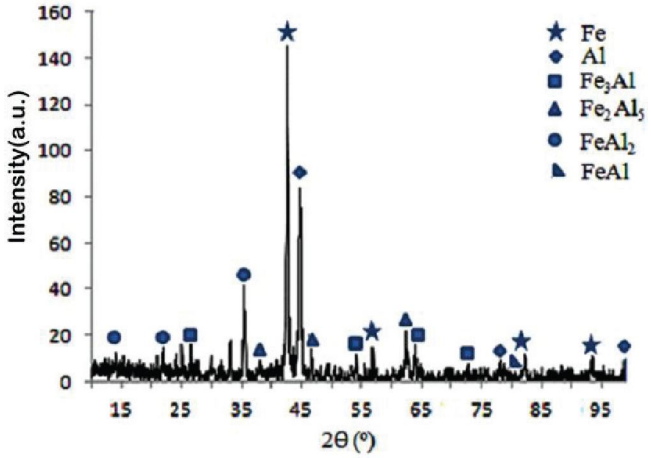
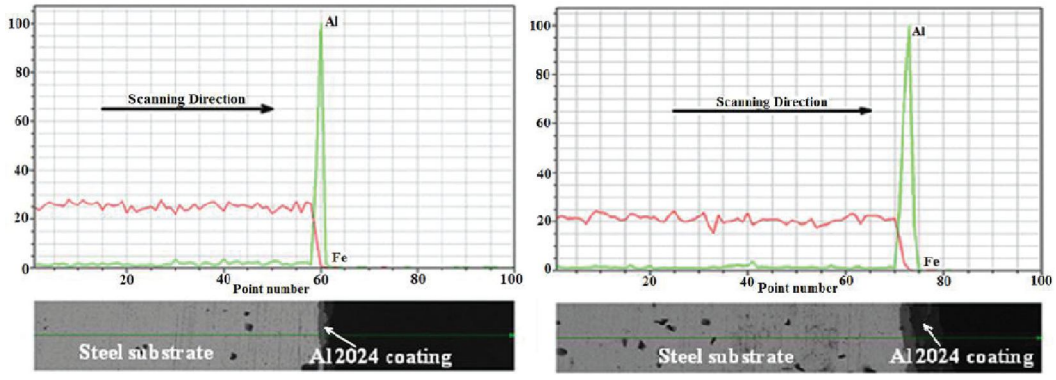
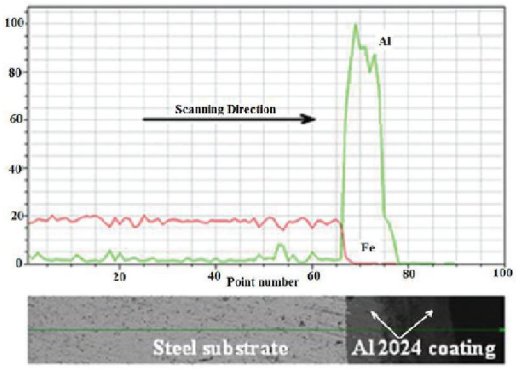


Figure 2. XRD patterns of steel substrates coated with Al2024 powders in a planetary ball mill

Fig. 3 shows the cross-section microstructures and main element distributions of the steel substrates with Fe-Al coatings produced under different milling times of 2h (Fig. 3a), 6h (Fig. 3b), and 10h (Fig. 3c). The EDX line scans were performed along the arrow lines marked in Fig. 3 from the inner substrate to the top coating surface. As shown in Fig 3a, the discontinuous and thin diffusion layers were formed on the steel surface at the beginning of the formation of Fe-Al coating. Mechanical milling process made the substrate surface to be more activated. Therefore, the steel surface was easier to be diffused and deposited by Al atoms. The initial diffusion layer of Fe-Al deposited a foundation for the following deposition of coating. The thickening mechanisms of depositing coating were substantiated with highly activated surfaces. Thicker Fe-Al coating was deposited on the surface of steel substrate (Fig. 3b). A flaking phenomenon occurred on the coating surface due to the repeated affects of ball milling during mechanical milling process. After a milling time of 10h, highest coating thickness was finally obtained on the surface of steel substrate (Fig. 3c). Moreover, the diffusion layer generally showed a gradual change of Al element concentrations. When the milling time was 10h, approximately 200 μm thickness of Fe-Al coating was deposited on the steel substrate through the mechanical milling process (Fig. 3c).



(a) (b)

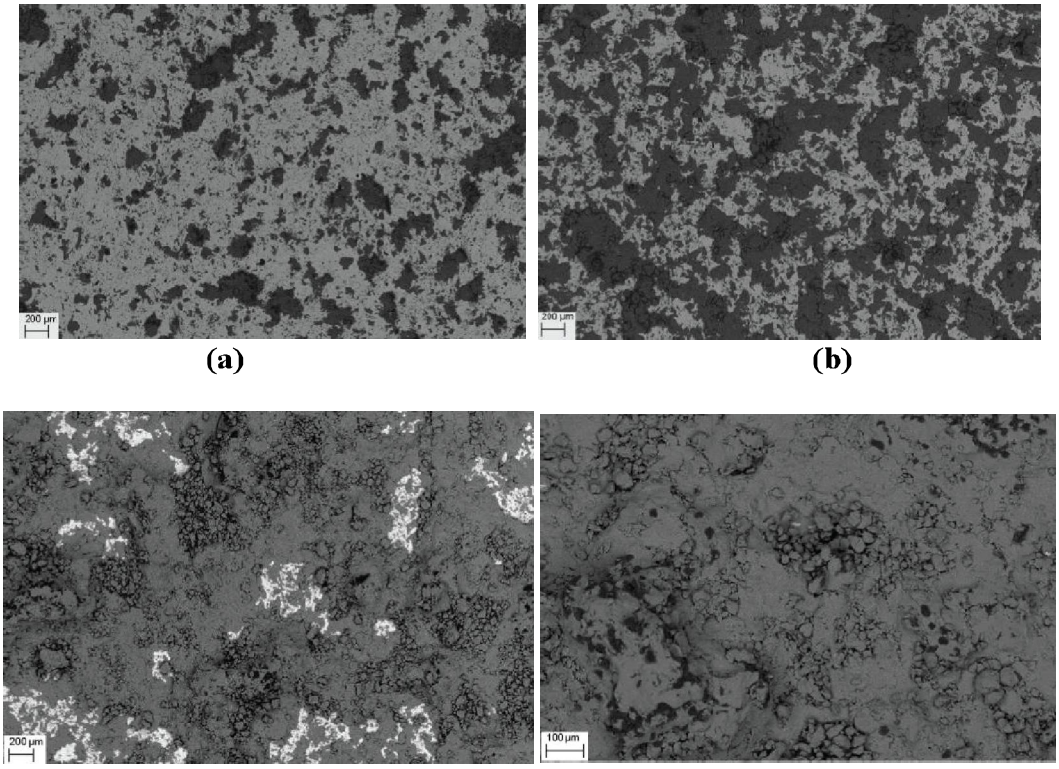


(c)

Figure 3. Cross-section images by SEM and EDX element line scan on Fe-Al coatings prepared using the same rotation speed (400 rpm) and the different milling times of 2h (a), 6h (b), and 10h (c)

3.2. Morphological evaluations

Fig. 4 shows the surface morphologies of the Fe-Al coating at 300 rpm. In the initial stage of milling, ductile Al 2024 powders are subjected to ball-powder-ball and ball-steel substrate-ball collisions. As can be seen in Fig. 4a, dark fields show deposition region of Al 2024 powders while light fields show the steel surface. In the second stage of milling, powders coated on the steel substrate are subjected to ball-steel substrate-ball collisions. Uncovered powders on the substrate tend to deposit on coating layer of the first stage due to ductile coating layer in this stage (Fig. 4b). Furthermore, cold welding process between ductile Al2024 particles is very important for coating process in the second stage (Fig 4b and Fig. 4c). In the final stage of milling, more homogeneous surface coating was obtained for Al 2024 particles (Fig. 4d).



(a) **(b)**

(c) **(d)**

Fig. 4. SEM images showing the characteristic morphologies of the top surfaces of the deposited coatings milling times at 300rpm: (a) 1h, (b) 4h, (c) 8h and (d) 10h

3.3. ANN modeling results

From the well known and widespread identification tools, the root mean squared error (RMSE) and the mean absolute percentage error (MAPE) values were calculated from Eqs.6 and 7 [11]. Models that produce the best estimated values were selected as the forecasting models.

$$RMSE = \sqrt{\frac{1}{N}\sum_{i=1}^{N}(t_i - td_i)^2} \quad (6)$$

$$\mathrm{MAPE} = \frac{1}{\mathrm{N}}\left(\sum_{\mathrm{i}=1}^{\mathrm{N}}\left[\left|\frac{\mathrm{t_i} - \mathrm{td_i}}{\mathrm{t_i}}\right|\right]\right)\times 100 \quad (7)$$

where t_i is the real value, td_i is the model prediction value and N is the number of testing data. Table 1 shows the actual values, degrees of deviation, percentage error rates, RMSE and MAPE calculated using the estimated models. The normalization (scaling) operations were carried out using Eq. 8:

$$\mathrm{X_{norm}} = 2\times\frac{\mathrm{X} - \mathrm{X_{min}}}{\mathrm{X_{max}} - \mathrm{X_{min}}} - 1 \quad (8)$$

where X_{norm} is the normalized value, X is the true value of the variable, X_{min} is minimum value of the data set and X_{max} is the maximum value of the data set.

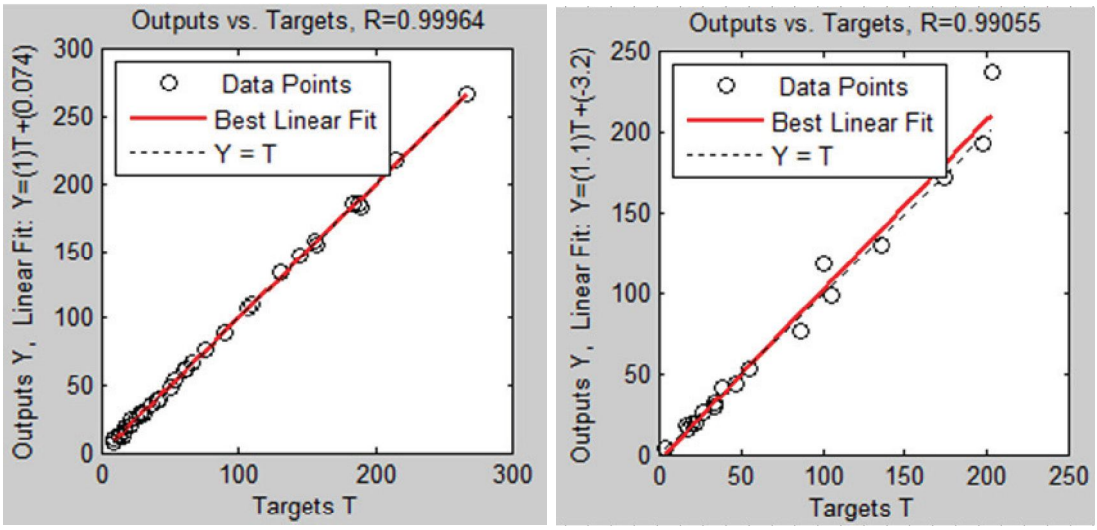
The predicted values, deviation and % error for the coating thickness on the steel substrate are provided in Tables 1 and 2.

Table 2. Experiment data and predicted output from the ANN network for testing

Sample ID	Milling Speed (rpm)	Particle Size (μm)	Milling Time (h)	Coating Thickness (μm)		
				Measured	Predicted	% Error
3	200	155	4	34	32.71	3.81
6	200	155	10	86	76.51	11.04
8	200	60	2	17	15.97	6.06
11	200	60	8	55	52.74	4.12
13	200	23	1	4	4.16	-4.12
16	200	23	6	34	29.50	13.22
19	300	155	1	20	19.07	4.63
22	300	155	6	105	98.72	5.98
27	300	60	4	27	26.74	0.96
30	300	60	10	174	172.34	0.95
32	300	23	2	16	17.92	-12.00
35	300	23	8	100	118.11	-18.11
38	400	155	2	47	43.72	6.99
41	400	155	8	203	238.24	-17.36
43	400	60	1	22	19.75	10.23
46	400	60	6	135	130.83	3.09
51	400	23	4	38	41.62	-9.51
54	400	23	10	198	193.65	2.20
MAPE				**7.466**		
RMSE				**10.001**		

However, several values were not as close as others, which was due to the errors caused by the material, the measurements and process parameters. These errors could be neglected given

that the learning level of the artificial neural network is 92.5 %. This study revealed that the predictions made using the ANN produced more accurate results. Fig. 5 shows the regression analysis of the ANN model for the volume loss, specific wear rate and surface roughness. The correlation coefficient was obtained to be 0.99, indicating good agreement between the experimental results and the model prediction (for training data set: $R_{\text{coating thickness}}$=0.99964 and for testing data set: $R_{\text{coating thickness}}$=0.99055).



(a) (b)

Figure 5. Regression analysis for the neural network responses and the target for the training data set (a) and the testing data set (b)

A comparative plot of these values was provided in Fig. 6. A comparison between the measured and predicted composite powder properties at the testing stage indicates a high correlation.

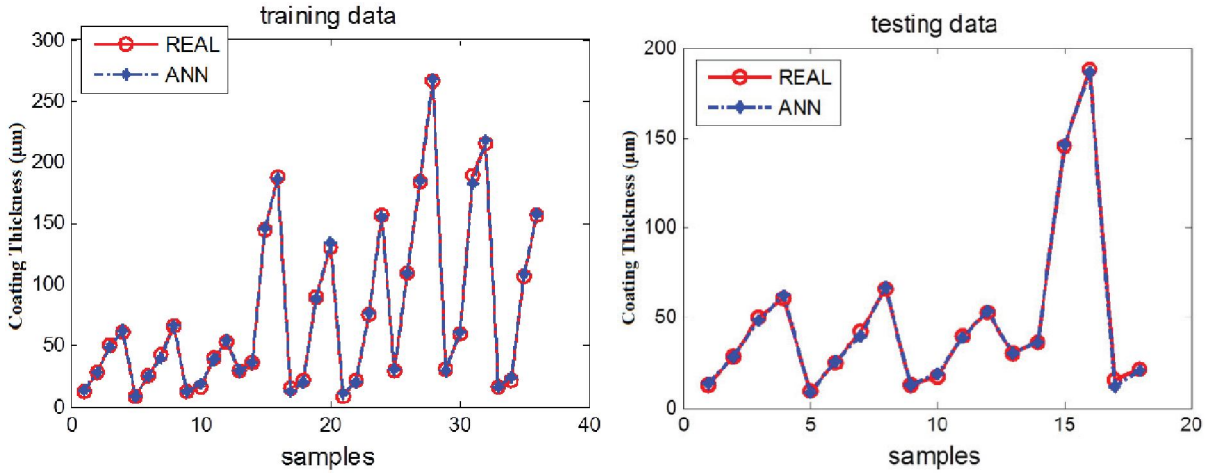


Figure 6. The comparison of measured values and ANN values for the (a) training data set (b) testing data set

4. CONCLUSIONS

The Fe-Al coatings were fabricated on the low carbon steel by mechanical alloying method. It was found that an increase in the applied milling time, the milling speed and size of milled powders affect the coating thickness. The deposition of a uniform coating by mechanical milling is possible, but it requires optimization of milling parameters and properties of as-

received powders so that the uniform distribution of ball-substrate-ball collisions over the processed surface is efficient. The coating thickness on the steel substrate increased with increasing milling time. The coating thickness increased to its maximum value after 10h of milling. The ANN model generated satisfactory results with high correlation coefficients. The mean absolute percentage error (MAPE) for predicted values did not exceed 7.466%. Therefore, using ANN model, results can be estimated satisfactorily which thereby reduces the testing time and cost.

Acknowledgements
The authors are grateful to the Karadeniz Technical University Research Fund for financially supporting this research (No: BTAP-9582). The researchers would also like to thank the Gundogdu Exotherm Service for providing the Al 2024 powders.

REFERENCES

1. Zhan Z, He Y, Wang D, Gao W (2006) Low-temperature processing of Fe-Al intermetallic coatings assisted by ball milling. Intermetallics 14:75-81.
2. Canakci A, Ozsahin S, Varol T (2012) Modeling the influence of a process control agent on the properties of metal matrix composite powders using artificial neural networks. Powder Technol 228:26-35.
3. Guessasma S, Montavon G, Gougeon Patrick, Coddet C (2003) Designing expert system using neural computation in view of the control of plasma spray processes. Mater Des 24: 497-502.
4. Çetinel H, Öztürk H, Çelik E, Karlık B (2006) Artificial neural network-based prediction technique for wear loss quantities in Mo coatings. Wear 261:1064-1068.
5. Rashidi AM, Hayati M, Rezaei A (2012) Application of artificial neural network for prediction of the oxidation behavior of aluminized nano-crystalline nickel. Mater Des 42: 308-316.
[6] Guessasma S, Coddet C (2004) Microstructure of APS alumina-titania coatings analysed using artificial neural network. Acta Mater 52:5157-5164.
[7 Pham DT, Liu X (1995) Neural Network for Identification, Prediction and Control. 2nd printing, Springer-Verlag, London.

[8] Zhang C, Kanta AF, Li CX, Li CJ, Planche MP, Liao H, Coddet C. (2009) Effect of in-flight particle characteristics on the coating properties of atmospheric plasma-sprayed 8 mol% Y_2O_3–ZrO_2 electrolyte coating studying by artificial neural Networks. Surf Coat Int 204:463-469.
[9] Hayajneh M, Hassan AM, Alrashdan A, Mayyas AT (2009) Prediction of tribological behavior of aluminum-copper based composite using artificial neural network. J Alloys Compd 470:584-588.
[10] Urakaev FK, Boldyrev VV (2000) Mechanism and kinetics of mechanochemical processes in comminuting devices: 2. Applications of the theory. Experiment. Powder Technol 107:197-206.
[11] Canakci A, Varol T, Ozsahin S (2013) Analysis of the effect of a new process control agent technique on the mechanical milling process using a neural network model: Measurement and Modeling, Measurement 46:1818-1827.